Microrheology of Microtubule Solutions and Actin-Microtubule Composite Networks

Vincent Pelletier, Naama Gal, Paul Fournier, and Maria L. Kilfoil*

Department of Physics, McGill University, Montréal, Canada H3A 2T8

(Received 1 September 2008; published 7 May 2009)

We perform local or microrheological measurements on microtubule solutions, as well as composite networks. The viscoelastic properties of microtubules as reported from two-point microrheology agree with the macroscopic measurement at high frequencies, but appear to show a discrepancy at low frequencies, at time scales on the order of a second. A composite of filamentous actin (F-actin) and microtubules has viscoelastic behavior between that of F-actin and pure microtubules. We further show that the Poisson ratio of the composite, measured by the length-scale dependent two-point microrheology, is robustly smaller than that of the F-actin network at time scales $\tau > 1$ s, suggesting that a local compressibility is conferred by the addition of microtubules to the F-actin network.

DOI: 10.1103/PhysRevLett.102.188303 PACS numbers: 83.80.Lz, 83.60.Bc, 87.15.La, 87.16.Ka

The mechanics of living cells is determined by the mechanical behavior of the composite cytoskeleton of actin filaments, intermediate filaments, and microtubules, along with associated proteins that can bundle or crosslink each type of filament, transport cargo along them, and control their length via polymerization dynamics. A question of intense interest is how the cytoskeleton transduces tensile and compressive forces generated by the motors and polymerizing machines to perform fundamental cell functions such as cell motility and cell division.

Because the cell is highly dynamic and heterogeneous, determining its mechanical properties is challenging. The overall stiffness of the cell has been measured using a variety of methods *in vivo* [1]. A bottom-up *in vitro* approach involving individual reconstituted actin filaments in a controlled environment, where filament length and applied external stress (to mimic internal forces) may be tuned, has been used to construct a minimal model for cell mechanics whose nonlinear viscoeleastic response can reproduce the stiffness of cells [2–4].

The contributions of microtubules and intermediate filaments to cell mechanics are missing from this picture. While different modes of regulatory and structural interactions between actin-based motor proteins and both microtubules and microtubule-based motor proteins have been proposed [5], intriguingly, it has been shown that the different filament types influence each other by virtue of their presence through their respective viscoelastic responses [6]. Actin filaments are a prototypical example of semiflexible polymers, and entangled, uncrosslinked actin filaments have been shown to follow the wormlike-chain model [2,3,7]. Microtubules are the stiffest elements in cells. Their fluctuations, although much smaller than those of actin filaments, are important for deployment of polymerization forces and for the search and capture mechanism used to position the mitotic spindle [8]. They have a persistence length of a few mm [9], and in solution might be expected to behave as rigid rods. Macroscopic linear rheology of microtubule solutions has shown an elastic plateau modulus of $\sim$1 Pa, with a weak frequency dependence and no terminal relaxation over a frequency range extending as low as $\omega = 6.3 \times 10^{-3}$ rad/s [10]. This behavior does not conform to existing theory of rotational motion of rods often used to fit these experiments [11]. A more detailed description, which contains an improved theory of the reorientational events [12], shows that the effective times scales are considerably slower than originally predicted. Nevertheless, the elastic modulus reported by the bulk experiments is at least an order of magnitude higher than expected from a plateau modulus of entropic origin arising from rigid rod number density, or from entanglements of microtubules behaving as semiflexible polymers. Surprisingly, to date there have been no attempts to use local probes of viscoelasticity *in vitro* in microtubule solutions. One significant challenge is that for the magnitude of elastic modulus and the 1.5 μm mesh size the solutions exhibit, the fluctuations probed by the beads would be expected to be sufficiently small that the cross-correlated bead motions would be at or below the limit of the uncertainty in the measurement attainable by previous microrheology experiments.

In this Letter, we use one-point (1P) and two-point (2P) microrheology to probe the mechanical properties of microtubule solutions and a composite network of microtubules and filamentous actin (F-actin). Linear viscoelastic behavior can be quantified by the complex shear modulus G^*, separable into elastic and viscous moduli, $G^*(\omega) = G'(\omega) + iG''(\omega)$. The method of passive microrheology employs the thermalized dynamics of micron-sized tracer beads to extract $G^*(\omega)$ [13]. The use of the autocorrelated motion of many individual beads to obtain $G^*(\omega)$ is an effective probe of local dynamics in homogeneous systems. Pairwise correlated motions can also be used to extract $G^*(\omega)$ with a probed length scale on the order of 5–100 μm, intermediate between those of the bead radius a and the macroscopic experiment. The relaxations probed

by microrheology depend on the nature of the bead coupling to the thermal fluctuations, and this can be exploited to use the 1P and 2P methods to probe length-dependent effects [2,3]. We exploit it here to observe and investigate an apparent relaxation during the experimental window that is not probed by the bulk rheology, and to investigate the mechanical properties of a model composite cytoskeleton at length scales relevant for the cell.

Preparations of the microtubule and F-actin–microtubule composite networks and beads are described in [14]. Example fluorescence images of a typical MT solution and composite network are shown in Figs. 1(a) and 1(b). Polystyrene particles are pretreated [15] and chosen to have diameters larger than the material mesh size, to approximate a microscopic continuum condition. Particles of radius $a = 0.95$ μm are used for MT solutions and composite networks, and $a = 0.5$ μm for F-actin.

Following equilibration, the sample is imaged in bright field with an inverted microscope (objective: 63X; NA = 1.4, oil), at ~40 μm depth so that wall effects may be neglected. To image particle motions, 6000 frames are acquired at 16 frames/sec and 1 ms exposure time. Particle positions are identified through feature finding algorithms to better than 20 nm resolution and their trajectories determined [16] to calculate the ensemble averaged mean squared displacement (MSD), $\langle \Delta r^2(\tau) \rangle$. Overall center of mass motion of all the particles in each field of view is removed. All analysis is performed in MATLAB.

Using the generalized Stokes-Einstein relation (GSER), we interpret MSDs to obtain a good approximation of the viscoelasticity probed by 1P microrheology. The scaled MSD for MTs shown in Fig. 1(c) evolves as a Newtonian fluid at short times, and reaches a plateau at intermediate times. The corresponding 1P apparent moduli [Fig. 1(d)] show elastic plateau behavior at intermediate frequencies with magnitude 0.1 Pa, an order of magnitude lower than that measured by macroscopic rheology, and crossover to viscous behavior at high frequency. The MT solution displays 1P apparent moduli qualitatively similar to those we observe for F-actin at 1.0 mg/mL, analyzed for comparison.

We probe microscopic length scales larger than a using 2P microrheology. We calculate the tensor of pairwise cross-correlated bead displacements as a function of separation r and lag time τ, and the component in the direction of bead separation, $D_{rr}(r, \tau)$, is used to extract $G^*(\omega)$ [13]. For correlated long wavelength thermal fluctuations in a homogeneous medium, $D_{rr} \sim 1/r$ [13], and $rD_{rr}(\tau)$ is used in the GSER to extract the approximate viscoelastic modulus. The range of r over which $D_{rr} \sim 1/r$ is typically 10–50 μm. We are able to measure bead correlated motions as small as 1.7×10^{-5} μm^2, enabling sensitivity to the very small fluctuations of the MTs via the 2P method. We show the 2P dynamics in Fig. 2(a). The MTs solution shows dramatically different behavior from the 1P microrheology, with $rD_{rr}(\tau)$ evolving as an elastic solid at short times, crossing over to evolution resembling a relaxation at long times. Although $rD_{rr}(\tau)$ is much noisier for the MTs

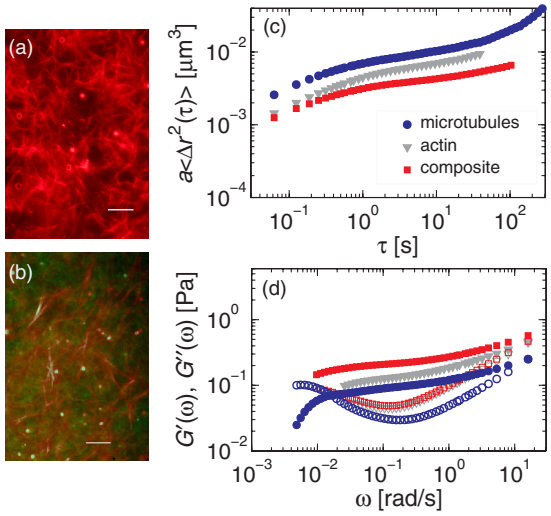

FIG. 1 (color online). (a),(b) Fluorescence images of (a) a typical 2.4 mg/mL labeled MT solution and (b) a typical composite network of MTs (2.4 mg/mL) and F-actin (1.0 mg/mL). Color was added following image capture. Scale bars are 10 μm. (c) MSD scaled by the bead size for a 2.4 mg/mL MT solution (blue ○), a 1.0 mg/mL F-actin (gray ▽) network, and a composite MT and F-actin network at same concentrations (red squares). (d) Corresponding 1P $G'(\omega)$ (solid symbols) and $G''(\omega)$ (open symbols).

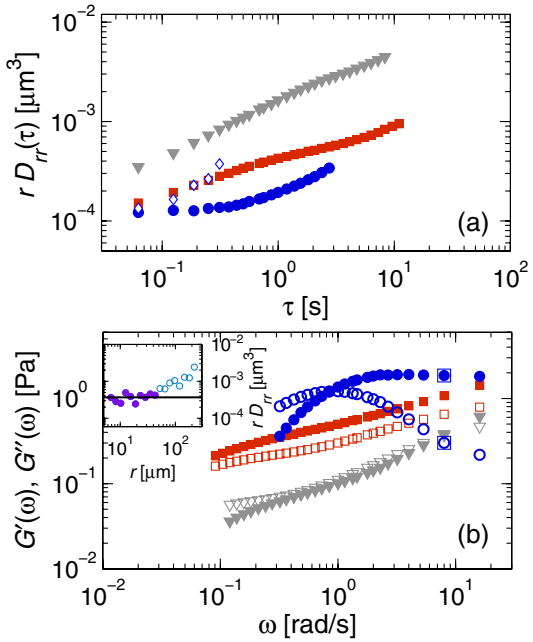

FIG. 2 (color online). $rD_{rr}(\tau)$ (a) and 2P apparent moduli (b) for the same MT solution, F-actin network, and composite MT and F-actin network samples as shown in Fig. 1(c). Small ◇ are unlabeled MT solution. Inset: fit of rD_{rr} to constant at lag time corresponding to $\omega = 8.0$ rad/s, used to obtain the data for $G^*(\omega)$. Fit is performed over solid symbols; open symbols are outside the range $D_{rr} \sim 1/r$.

than for the F-actin (already inherently noisy), the data are robust, as demonstrated in the inset of Fig. 2(b). The 2P microrheology is shown in Fig. 2(b). The high frequency plateau apparent elastic modulus for MTs, at ~2 Pa at 10 rad/s, is larger than that of F-actin, and exhibits a sharp crossover to predominantly viscous behavior at low frequencies that is not observed in the F-actin. The actin 2P microrheology scales with a power-law between 1/2 and 3/4 for $\tau < 1$ s, in agreement with earlier results [2,13]. Our MT system could differ, for example, in degree of polymerization, from prior macrorheology studies [10]; however, the magnitude of G' inferred from 2P microrheology is comparable to what is reported there.

In unlabeled MT solutions, we find this relaxation occurs at even higher frequency. In this case, at the smallest separations probed, $D_{rr}(r)$ decays faster than the expected $1/r$. To determine whether this is the source of the relaxation observed at the 2P length scale that is not reported in the bulk rheology, we bin the $D_{rr}(r,\tau)$ signal at finer resolution in r. The results for $\tau = 0.063$ s and 0.25 s, shown in Fig. 3, display the faster decay of $D_{rr}(r)$ at short r, and the limit of the uncertainty in the measurement at large r. We naturally ask whether the faster-than-$1/r$ decay is a propagating mode. A propagating and diffusive mode should appear at larger r at a rate scaling as $t^{1/2}$. In the inset of Fig. 3, the crossover distance r_c between the faster decay and the region of $1/r$ behavior is shown to depend weakly or not at all on τ. The anomalous correlations do not appear to be a propagating mode, at least not beyond ~15 μm, and are not the source of the relaxation observed in the 2P microscopic rheology. We can extract rD_{rr} robustly for each τ directly by fitting only to the $1/r$ regime at intermediate r. The points thus obtained are shown as diamonds in Fig. 2(a). At the shortest time probed, the bead correlated motions are larger than those in labeled MTs, although the difference is within the sample-to-sample variation. As $rD_{rr}(\tau)$ evolves, the onset of relaxation is faster in this case where the beads couple less efficiently to the MTs. However, our 2P microrheology results for both MT systems differ at low frequency from prior reports of macrorheology [10], suggesting a real discrepancy between the microscopic and macroscopic rheology.

Since we observe this relaxation in the 2P microrheology on length scales relevant for the cell environment, we investigate whether we might expect it to be directly relevant to cells. To do this, we analyze a composite sample prepared with both MTs and F-actin. In the composite network, $D_{rr}(r)$ does not exhibit the decay faster than $1/r$ at short r, as shown in Fig. 4. Instead, $D_{rr}(r)$ for both the composite and F-actin sample, also shown in Fig. 4, shows remarkably robust $1/r$ behavior over the entire range of lengths probed.

We also compare the 1P and 2P microrheology of the composite with the microrheology of F-actin and MT solutions. At the length scale of the individual beads probed by the 1P microrheology, shown in Fig. 1, the composite appears very similar mechanically to F-actin. This might be expected for the smaller F-actin mesh size of ~0.3 μm [2], and, by extension, closer coupling between the beads and the actin filaments. At the length-scale of the bead separation probed by the 2P technique, shown in Fig. 2, the mechanical behavior of the composite is qualitatively different from that of MTs. The composite does not exhibit the sharp relaxation, although, interestingly, the apparent modulus at high frequency is approximately the same. The composite apparent modulus is more dominantly elastic and is larger in magnitude by roughly an order of magnitude over that of F-actin, and if the decay may be viewed as tending towards agreement with the 1P modulus at low frequencies, as is observed in F-actin, the time scale for the decay is a factor of 10–30 longer. In cells, the presence of surrounding F-actin has been shown to reduce the length scale for transverse fluctuations of MTs [6]. It is therefore interesting to ask whether the presence of MTs modulates actin filament fluctuations.

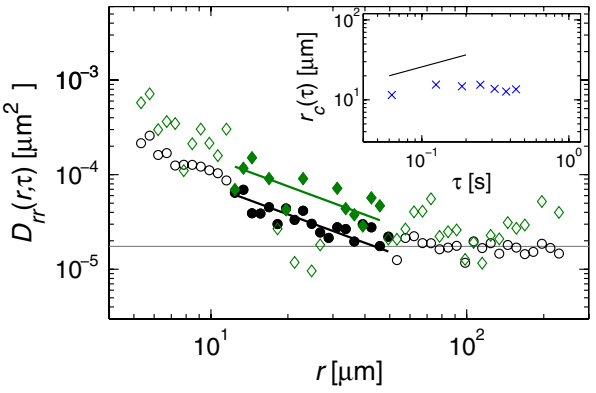

FIG. 3 (color online). D_{rr} for unlabeled actin sample at $\tau = 0.063$ s (black ○) and $\tau = 0.25$ s (green ◇). The noise floor in D_{rr} is 1.7×10^{-5} μm^2 at $\tau = 0.063$ s (gray line). Solid symbols identify the points used to fit to $1/r$ (lines). Inset: Length scale above which cross correlations decay as $1/r$. The line is a guide to the eye with slope 1/2.

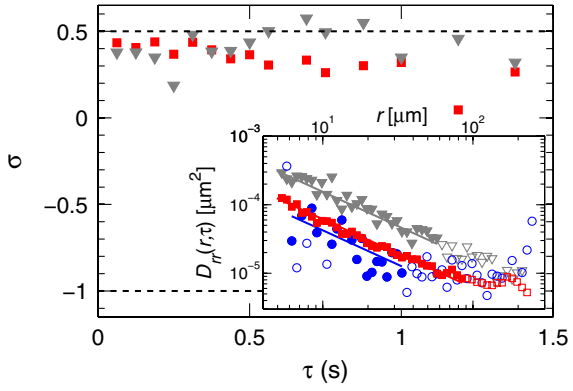

FIG. 4 (color online). Poisson ratio for composite MT-actin (red squares) and F-actin (gray ▽) network. Inset: D_{rr} for F-actin (gray ▽), composite (red squares) and labeled MT solution (blue ○) at $\tau = 0.19$ s.

In pure F-actin at this concentration, the difference between the 1P and 2P rheology, and the convergence of the two at low frequency, was explained by a model for semiflexible polymers in which density fluctuations decay diffusively along the filament the distance of the persistence length l_p; this relaxation is probed by both the macroscopic and 2P microscopic rheology [2]. In that model, the time scale for density fluctuations to diffuse l_p is $\tau_p \approx (l_p/l_e)^2\tau_e$ [7,17], where l_e and τ_e are the entanglement length and time, respectively. For the time scale to increase by more than a decade would require either a decrease in l_e by a factor of 3–5 from pure F-actin, by which a tenfold increase in the 1P modulus would be expected [18] compared to the twofold increase observed, or greater persistence in the actin filament transverse fluctuations within the surrounding MTs. However, in the model the time scales for decay are only scaling predictions to within a numerical prefactor that could differ significantly from unity, and more direct tests are needed.

The ratio between the pairwise in-phase perpendicular and parallel cross correlated motions $D_{\theta\theta}(r,\tau)$ and $D_{rr}(r,\tau)$ depends on the Poisson ratio σ [19]. The data for $D_{\theta\theta}(r,\tau)$ and $D_{rr}(r,\tau)$ are remarkably robust in both F-actin and the composite network, and permit measurement of σ at each τ, shown in Fig. 4. We find that for F-actin, $\sigma \simeq 1/2$, as reported previously [2]. By contrast, in the composite network, σ is unambiguously less than $1/2$ at longer times, and is closer to 0.3. At a macroscopic, continuum level, a solution such as this is not expected to be compressible. Given the stiffness and length of MTs, the deviation from $1/2$ of σ upon the addition of MTs to F-actin suggests interpretation of Fig. 4 in terms of a local compressibility for the composite network. That this can appear in the length-scale dependent microscopic rheology at the tens of μm range may be interesting and relevant for the cytoskeleton.

We have used microrheology to probe biologically relevant length scales of a few tens of μm on time scales of seconds in MT solutions and composite networks of F-actin and MTs. We have shown that probing the MTs system on these length scales reveals local relaxations not reflected in the macrorheology. The addition of F-actin to the MT solution enhances the coupling of the beads to the material, and the very robust data that may then be obtained reveals intriguing differences in the material properties of the composite from either MTs or F-actin. This work establishes a starting point for microrheology on composites of cytoskeletal filaments, and we anticipate applying this technique to composites with added MT polymerizing machines and motors, agents that change the filament dynamics, to measure the cytoskeleton mechanics during these important cellular transitions.

The authors wish to thank F. MacKintosh, A. Maggs, and D. A. Weitz for helpful comments, and D. Cooper, A. Orth, and D. Foreman-Mackey for technical assistance. This work was supported by the Natural Sciences and Engineering Research Council of Canada (NSERC).

*kilfoil@physics.mcgill.ca

[1] B. D. Hoffman, G. Massiera, K. M. van Citters, and J. C. Crocker, Proc. Natl. Acad. Sci. U.S.A. **103**, 10 259 (2006).
[2] M. L. Gardel, M. T. Valentine, J. C. Crocker, A. R. Bausch, and D. A. Weitz, Phys. Rev. Lett. **91**, 158302 (2003).
[3] J. Liu, M. L. Gardel, K. Kroy, E. Frey, B. D. Hoffman, J. C. Crocker, A. R. Bausch, and D. A. Weitz, Phys. Rev. Lett. **96**, 118104 (2006).
[4] D. Mizuno, C. Tardin, C. F. Schmidt, and F. C. MacKintosh, Science **315**, 370 (2007); M. L. Gardel, F. Nakamura, J. Hartwig, J. C. Crocker, T. P. Stossel, and D. A. Weitz, Phys. Rev. Lett. **96**, 088102 (2006).
[5] O. Rodriguez, A. Schaefer, C. M. Mandato, P. M. Forscher, W. M. Bement, and C. M. Waterman-Storer, Nat. Cell Biol. **5**, 599 (2003).
[6] C. P. Brangwynne, F. C. MacKintosh, S. Kumar, N. A. Geisse, J. Talbot, L. Mahadevan, K. K. Parker, D. E. Ingber, and D. A. Weitz, J. Cell Biol. **173**, 733 (2006).
[7] F. C. MacKintosh, J. Käs, and P. A. Janmey, Phys. Rev. Lett. **75**, 4425 (1995).
[8] A. Desai and T. J. Mitchison, Annu. Rev. Cell Dev. Biol. **13**, 83 (1997).
[9] F. Pampaloni, G. Lattanzi, A. Jonas, T. Surrey, E. Frey, and E.-L. Florin, Proc. Natl. Acad. Sci. U.S.A. **103**, 10 248 (2006).
[10] M. Sato, W. H. Schwartz, S. C. Selden, and T. D. Pollard, J. Cell Biol. **106**, 1205 (1988); Y.-C. Lin, G. H. Koenderink, F. C. MacKintosh, and D. A. Weitz, Macromolecules **40**, 7714 (2007).
[11] M. Doi and S. Edwards, *The Theory of Polymer Dynamics* (Oxford University Press, Oxford, 1986).
[12] O. D. Brazhnik and A. R. Khokhlov, Proc. SPIE Int. Soc. Opt. Eng. **1402**, 70 (1991).
[13] J. C. Crocker, M. T. Valentine, E. R. Weeks, T. Gisler, P. D. Kaplan, A. G. Yodh, and D. A. Weitz, Phys. Rev. Lett. **85**, 888 (2000).
[14] See EPAPS Document No. E-PRLTAO-102-036921 for text describing preparations of the microtubule and actin-microtubule composite networks, and pretreatment of beads to prevent nonspecific interaction with the proteins. For more information on EPAPS, see http://www.aip.org/pubservs/epaps.html.
[15] S. Faraasen, J. Vörös, G. Csúcs, M. Textor, H. P. Merkle, and E. Walter, Pharm. Res. **20**, 237 (2003).
[16] J. C. Crocker and D. G. Grier, J. Colloid Interface Sci. **179**, 298 (1996).
[17] A. C. Maggs, Phys. Rev. E **55**, 7396 (1997); D. C. Morse, Macromolecules **31**, 7044 (1998).
[18] I. Y. Wong, M. L. Gardel, D. R. Reichman, E. R. Weeks, M. T. Valentine, A. R. Bausch, and D. A. Weitz, Phys. Rev. Lett. **92**, 178101 (2004).
[19] A. J. Levine and T. C. Lubensky, Phys. Rev. Lett. **85**, 1774 (2000).